Available online at www.sciencedirect.com
SCIENCE DIRECT®
Journal of Nuclear Materials 354 (2006) 163–170
journal of nuclear materials
www.elsevier.com/locate/jnucmat

Deposition behaviour of corrosion products on the Zircaloy heat transfer surface

Jei-Won Yeon [a], Yongju Jung [a], Su-Il Pyun [b,*]

[a] *Nuclear Chemistry Research Division, Korea Atomic Energy Research Institute, P.O. Box 105, Yuseong-gu, Daejeon 305-600, Republic of Korea*
[b] *Department of Materials Science and Engineering, Korea Advanced Institute of Science and Technology, 373-1, Guseong-dong, Yuseong-gu, Daejeon 305-701, Republic of Korea*

Received 17 February 2006; accepted 31 March 2006

Abstract

The deposition behaviour of corrosion products on the Zircaloy heat transfer surface was examined under four different experimental environments. First, iron oxide deposition on two kinds of Zircaloy surfaces was carried out in order to evaluate the effects of the oxidation state of Zircaloy. Second, the amount of iron oxide deposits on the Zircaloy surface was measured in order to analyse the influence of dissolved hydrogen. Third, nickel oxide deposition was carried out on two Zircaloy surfaces with dense and porous iron oxide layers, respectively, to evaluate the effects of pre-deposited iron oxides. Finally, the effects of Fe^{2+} ions on the deposition of iron oxide micro-particles were examined in a suspended hematite solution and a mixed solution containing Fe^{2+} ions and suspended hematite. In our results, a heat treatment of the Zircaloy surface was effective for reducing the iron oxide deposition. Dissolved hydrogen and Fe^{2+} were found to promote the deposition of the iron oxides. And the amount of nickel oxide deposits was increased on the porous iron oxide layer.
© 2006 Elsevier B.V. All rights reserved.

1. Introduction

Corrosion products released from reactor structural materials, such as Inconel and stainless steel, are deposited on the surfaces of both the fuel cladding and the primary reactor system (e.g., steam generator). It is well known that the deposition phenomena of the corrosion products depend greatly on the type of nuclear reactor. In a BWR (boiling water reactor), most corrosion products are deposited on the fuel cladding through a so-called ‘boiling-promoted deposition’ mechanism and are activated to generate a radioactive ‘fuel CRUD (Chalk River unidentified deposits)’ that is generally referred to as the CRUD formed on the fuel cladding. In a PWR (pressurised water reactor) operated under a short-term fuel cycle program of 12 months, on the contrary, most corrosion products are observed in the steam generator. For these reasons, whereas the study of the fuel CRUD has not been considered an important issue in a PWR, it has long been recognised as a critical issue in a BWR and, accordingly, related research has been intensively carried out. Recently, however, extended burn-up

---

[*] Corresponding author. Tel.: +82 42 869 3319; fax: +82 42 869 3310.
E-mail address: sipyun@webmail.kaist.ac.kr (S.-I. Pyun).

0022-3115/$ - see front matter © 2006 Elsevier B.V. All rights reserved.
doi:10.1016/j.jnucmat.2006.03.017

programs for a long-term fuel cycle of 18–24 months have been introduced in many PWR plants since it became clear that a long-term fuel cycle operation has important benefits such as providing a more stable electric power supply and allowing for a reduction of the spent fuel. However, after applying the long-term fuel cycle program, safety concerns have arisen due to a considerable increase of the fuel CRUD. It has been reported that the fuel CRUD contributes to the occurrence of an AOA (axial offset anomaly) and an increase in the dose rate [1,2].

At present, approaches to mitigate the fuel CRUD problem can be categorised into two types. One method involves minimizing the release of corrosion products from reactor structural materials in order to reduce the formation of the fuel CRUD. To this end, various techniques such as a higher pH operation, use of EBA (enriched boric acid), hydrogen injection, and improvement of the cladding material have been investigated [2–4]. The other approach is to directly remove the fuel CRUD from the fuel cladding using numerous techniques involving a chemical purification, injection of zinc ions, magnetic separation, and an ultrasonic cleaning of the fuel [5–7].

Fundamental research on topics such as physicochemical characteristics of the fuel CRUD and a mechanistic study on the formation of the fuel CRUD has been actively undertaken. In particular, the formation study of nickel ferrite ($Ni_xFe_{3-x}O_4$), which is known to be the main component of fuel CRUD, is an important subject in relation to reactor coolant chemistry. Notably, thermodynamic evaluation results demonstrate that nickel ferrite is spontaneously formed by an exchange reaction between Ni^{2+} in the coolant and Fe^{2+} in the Fe_3O_4 lattice [8]. However, the formation mechanism of the nickel ferrite on the fuel cladding has not been clearly identified.

The present study focuses on an analysis of the formation process of fuel CRUD, i.e., the deposition process of the corrosion products, in order to obtain a better understanding of the origin of a fuel CRUD formation. The deposition behaviour of corrosion products on a Zircaloy heat transfer surface was examined under four discretely different experimental environments. First, an iron oxide deposition on two kinds of Zircaloy surfaces was carried out in order to evaluate the effects of the oxidation state of the Zircaloy surface. Second, the amount of iron oxide deposits on the Zircaloy surface was measured in an aqueous solution containing ferrous acetate to analyse the influence of the dissolved hydrogen in the following two conditions: (i) in a deaerated solution; and (ii) in a hydrogen-dissolved solution. Third, the effects of the iron oxide type on a nickel oxide deposition were analysed. Finally, a deposition of colloidal hematite particles was carried out to examine the effects of Fe ions on the deposition of an iron oxide microparticle in the following two kinds of solutions: (i) a suspended hematite solution; and (ii) a mixed solution containing Fe^{2+} ions and suspended hematite.

2. Experimental

2.1. Corrosion products

Ferrous ions (Fe^{2+}), nickel ions (Ni^{2+}), and colloidal hematite particles (< 0.5 μm in diameter) were chosen as the corrosion products to be tested. The sources of the Fe^{2+} and Ni^{2+} ions were ferrous acetate and nickel acetate, respectively. Suspended hematite solutions were prepared by thermal hydrolysis of a ferric solution. Test solutions used in this study consisted of at least one of the corrosion products and distilled water.

2.2. Deposition apparatus under subcooled boiling conditions

A high-temperature and high-pressure loop system was used for the deposition test under subcooled boiling. Fig. 1 shows the loop system, which was composed of a reactor, a rod-type heater installed within the reactor, a pressuriser, a heat exchanger, a circulation pump, and a chemistry control system. This loop system was designed such that the heat is transferred from the heater to the test solution, and at the same time the corrosion products were deposited on the surface of the rod-type heater. Four Zircaloy rods (Zircadyne-702, Wah Chang), the inside of which was filled with an electrically insulated heating coil and an insulator (e.g., MgO), were used as a rod-type heater (diameter = 12.7 mm, heat flux zone = 179 cm^2, maximum power = 1.25 kW) by which the solution temperature in the reactor was controlled. The pressure of the system was regulated by the pressuriser, which was filled with a condensed test solution and vapour at a high-temperature. During the deposition test, the solution was circulated within the loop

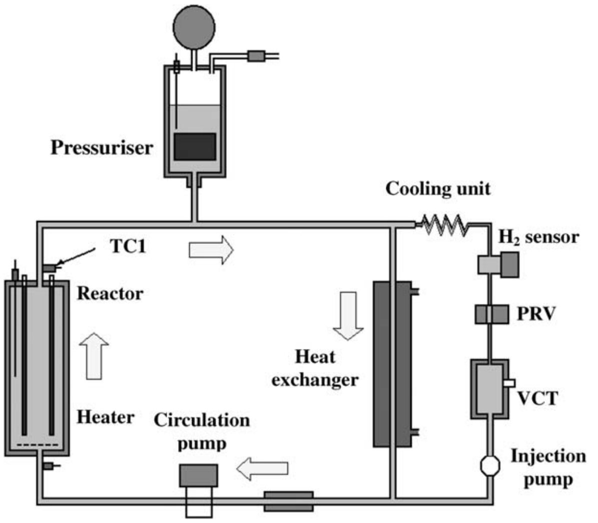

Fig. 1. Scheme of the high-temperature and high-pressure loop system.

system at 2.3 l/min using a circulation pump installed in the loop system, as shown in Fig. 1. Note that the calculated flow rate of the solutions along the fuel rod in the main reactor is about 3 mm/s.

The temperature profile of the test solutions with time, where the temperature was monitored with thermocouples (TC1 denoted in Fig. 1) near the outlet part of the reactor, consists of the following three periods: (1) the temperature is increased up to 300 °C; (2) the temperature is fixed during the prescribed time, defined as the 'deposition test time'; (3) the electric heater is turned-off immediately after the end of the second stage and the test solution is circulated until the solution temperature decreases to room temperature.

We devised a specific method for subcooled boiling, which is the heat transfer mode of a PWR in operation, given that it is difficult to induce subcooled boiling by use of only an electric heater with a relatively low power compared to that of a real fuel cladding. The main objective of the process is to rapidly decrease the pressure of the loop system so that small bubbles are generated on the heat transfer surface. The heat exchanger can take the heat energy from the loop system and it is used for a rapid reduction of the system pressure. The periodic operation of the heat exchanger provided the heat transfer surface with nearly continuous subcooled boiling during all the deposition tests.

In this study, three types of deposition tests were conducted under subcooled boiling conditions using the loop system. First, iron oxide deposition tests, both on a untreated Zircaloy polished with diamond paste and a heat-treated Zircaloy with steam of 400° to 500 °C for 4 h, were carried out in ferrous acetate solutions to elucidate the heat treatment effect of Zircaloy on the formation of the iron oxide deposits. Distillated water was used as steam source for the heat treatment of Zircaloy. Second, the iron oxide deposition on Zircaloy was investigated both in a hydrogen-dissolved ferrous acetate solution and in a deaerated ferrous acetate solution in order to analyse the effects of hydrogen on the formation of the iron oxide deposits. Molecular hydrogen was injected through the VCT (volume control tank) and the concentration of dissolved hydrogen was measured by a hydrogen analyser (Orbisphere 3600) installed in a bypass line of the loop system. Third, nickel oxide deposition tests on two kinds of iron oxide-coated Zircaloys were carried out in nickel acetate solutions so as to examine the effects of the iron oxide type on the nickel oxide deposition. The detailed experimental conditions of the deposition tests performed in this study are summarised in Table 1. The iron oxide deposits formed on the Zircaloy surface after the deposition tests were removed by ultrasonic cleaning in 5 M HCl solution. The iron concentration was determined by inductively coupled plasma-atomic emission spectrometry (ICP-AES) after completely dissolving the resulting solution in hot hydrochloric acid.

2.3. Deposition apparatus under non-boiling conditions

A once-through loop system was used for the deposition test under non-boiling conditions. Fig. 2 shows the once-through loop system, which is composed of a reactor, a rod-type heater installed within the reactor, a cooling unit, an injection pump, and a BPR (back-pressure regulator) valve. This system was designed so that the deposition behaviour of the corrosion products on the heat transfer surface such as that of a rod-type heater could be examined under non-boiling conditions; this means that all the test solutions exist in a liquid state within the reactor. One Zircaloy rod (diameter = 9.52 mm, heat flux zone = 75 cm^2, maximum power = 0.8 kW) with a structure similar to the Zircaloy rod used in the subcooled boiling conditions was installed in the center of the reactor. The pressure of the system was regulated by the BPR valve. During the deposition test, the test solution

Table 1
Experimental conditions of the iron and nickel oxide depositions

Test	Zry surface treatment	Iron oxide deposition (Step 1)			Nickel oxide deposition (Step 2)			
		Fe source	Deposition time (h)	T (°C)/P (kg/cm^2)	Ni source	DH (cm^3/kg)	Deposition time (h)	T (°C)/P (kg/cm^2)
Figs. 3, 4(a)	No	Fe(Ac[a])$_2$, 50 μg/ml Fe	0, 1, 2, 4, 8	215/34	Ni(Ac)$_2$ 30 μg/ml Ni, pH$_T$ = 7.0	36	12	300/160
Fig. 3	400–500 °C steam	Fe(Ac)$_2$, 50 μg/ml Fe	0, 1, 2, 4, 8	215/34	Ni(Ac)$_2$ 30 μg/ml Ni, pH$_T$ = 7.0	36	12	300/160
Fig. 4(b)	No	Fe$_3$O$_4$ particles, 0.92 μg/ml Fe	0, 3/2, 4, 12	100/boiling	Ni(Ac)$_2$ 20 μg/ml Ni, pH$_T$ = 7.0	36	12	300/160
Table 2	No	Fe(Ac)$_2$, 20 μg/ml Fe	10	300/160				
Fig. 6(a), Table 3	No	Suspended hematite, 30 μg/ml Fe, dia. < 0.5 μm	6	200/25				
Fig. 6(b), Table 3	No	Suspended hematite (30 μg/ml Fe, dia. < 0.5 μm) + Fe^{2+} ions 50 μg/ml Fe	6	200/25				

[a] Ac: CH$_3$COO$^-$.

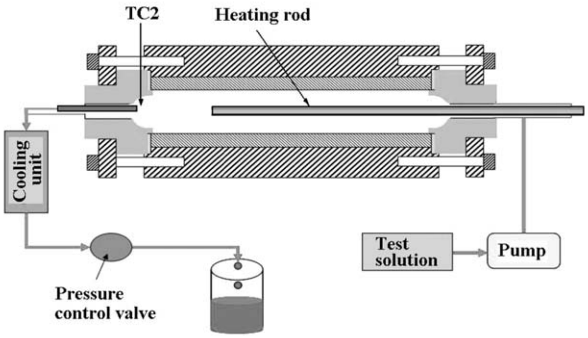

Fig. 2. Scheme of the high-temperature and high-pressure one-through loop system.

was supplied to the reactor at 10 ml/min using a injection pump installed in the loop system, as shown in Fig. 2. Note that the calculated flow rate of the solutions along the fuel rod in the main reactor is about 0.07 mm/s. The temperature profile of the test solutions with time was very similar to the profile described in Section 2.2, except that the solution temperature measured near the outlet part of the reactor (at TC2 in Fig. 2) is 200 °C.

The effect of Fe^{2+} ions on the deposition of hematite micro-particles was examined under non-boiling conditions using this loop system. As the iron oxide micro-particles were deposited on to the Zircaloy surface under subcooled boiling, the one-through loop system was utilised to remove the influence of a direct deposition of the micro-particles. The detailed experimental conditions of the deposition test are summarised in Table 1. The metal concentration of the deposits after the test was determined by the same method as described in Section 2.2.

3. Results and discussion

3.1. Heat treatment effect of the Zircaloy surface on iron oxide deposition

The surface of the fuel cladding is pretreated at the initial stage of an operation by increasing the temperature of the coolant in the power plant. This treatment forms a corrosion-resistive film on the fuel cladding, the chemical composition of which is mainly ZrO$_2$. It is well known that the zirconium oxide film has a remarkable stability in various chemical environments [9]. In order to determine the effect of this treatment on the deposition of Fe species, we performed iron oxide deposition tests with time on an untreated Zircaloy rod-type heater and on a heat-treated Zircaloy rod with steam at a temperature of 400–500 °C.

The deposition tests were carried out under subcooled boiling conditions in ferrous acetate solutions ([Fe] = 50 μg/ml) as corrosion products. We observed dark and dot-like deposits of iron oxides formed at specific sites on the Zircaloy surfaces after the deposition tests. The amount of deposits, which reflects the Fe amount within the deposits, was determined by ICP-AES after a removal of the deposits from the Zircaloy surfaces.

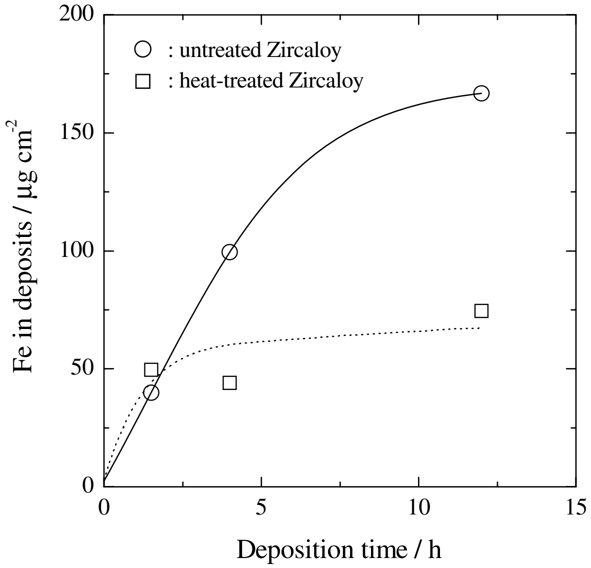

Fig. 3. Effects of a heat treatment of a Zircaloy surface on the deposition of iron oxide: solid line (○), untreated Zircaloy surface; dotted line (□), high-temperature heat-treated Zircaloy surface.

Fig. 3 shows that the deposition behaviour on the two Zircaloy surfaces, where the amount of deposits increased greatly with time, are very similar when the deposition test time is less than 2 h. However, when the deposition test time exceeds 4 h, distinctly different deposition behaviours were observed. Note that the deposition test time corresponds to the period of the second stage of the temperature profile described in Section 2.2. Specifically, the deposition rate decreased more sharply in the heat-treated Zircaloy, compared with the untreated Zircaloy. The amount of deposits on the untreated Zircaloy was about two times larger than that on the heat-treated Zircaloy at a deposition time exceeding 4 h, as shown in Fig. 3. This implies that a surface treatment of Zircaloy strongly influences the deposition behaviour of the Fe species as well as the deposition of the corrosion products generated in the PWR primary circuit.

3.2. Effect of dissolved hydrogen on the iron oxide deposition

Hydrogen gas is added to the primary coolant in order to protect the structural materials from the oxidizing species produced by water radiolysis [1,10]. Dissolved hydrogen is a unique chemical additive to control the redox condition in the coolant, and its optimal concentration is determined by evaluating its influence only on the removal of the oxidizing species as well as on the solubility of the metal oxides and PWSCC (primary water stress corrosion cracking) of steam generator tubing [10]. Therefore, in order to mitigate the current CRUD problem, it may also be necessary to estimate the effects of dissolved hydrogen on the deposition of the corrosion products.

Table 2
Effects of dissolved hydrogen on the iron oxide deposition on the heat exchanging Zircaloy surface in a ferrous acetate solution (20 μg/ml Fe) for 10 h at 300 °C

H_2 conc. (cm^3/kg)	Fe content in deposits (μg/cm^2)	
	Subcooled boiling	Non-boiling[a]
0	4.5	4.1
20	31.8	3.9

[a] Data of non-boiling tests were measured at 280 °C.

To examine the effects of dissolved hydrogen on the deposition of the Fe species, we performed deposition tests of Fe on Zircaloy in 20 μg/ml ferrous acetate solutions under subcooled boiling at 300 °C. Table 2 shows the amounts of Fe in the iron oxide deposited in 20 cm^3 H_2/kg hydrogenated and Ar gas-purged solutions, respectively. Iron oxide deposition was clearly promoted by the presence of dissolved hydrogen. However, no hydrogen effect was found under the non-boiling conditions tested at 280 °C.

It has been reported that the partial fraction of the hydrogen gas is higher inside the bubbles formed by water boiling [11]. This means that the hydrogen is more stable in the bubbles as a gaseous form and thus hydrogenated water may be boiled easier than pure water at the same temperature. In addition, the hydrogen concentration surrounding the vapour bubbles is clearly reduced. It has been reported that the iron oxide solubility is reduced with a decreased concentration of the dissolved hydrogen [9]. Given these experimental and reported results, it appears that dissolved hydrogen may affect the iron oxide deposition through the promotion of boiling process and by decreasing the local solubility of the iron oxide near the vapour bubbles.

3.3. Effect of pre-deposited iron oxide on the nickel oxide deposition

Nickel is always observed in deposits with iron oxide in the formation of a fuel CRUD. We measured the effects of iron oxide on the nickel oxide deposition in order to evaluate the reduction of the nickel content in the deposits through a control of the concentration of the Fe species.

Two different kinds of pre-deposited iron oxide layers were used for the deposition test: a uniform iron oxide layer deposited from Fe^{2+} ions at 215 °C and an inhomogeneous layer formed with magnetite particles at an 100 °C boiling. After deposition of the iron oxide layers, nickel oxide was deposited with Ni^{2+} ions for 12 h at 300 °C. Magnetite was selected as a pre-deposited iron oxide, because it is known to be the most stable iron oxide formed in a high-temperature aqueous solution [12].

Fig. 4(a) shows the relationship between the iron and nickel content in the mixed metal oxide deposits obtained after two sequential iron and nickel oxide deposition processes. The nickel oxide deposition was independent of the amount of pre-deposited iron oxide. This indicates that there was little interaction between the nickel oxide deposition and the pre-deposited iron oxide. Thus, it appears that the pre-deposited iron oxide layer formed from Fe^{2+} ions is so dense that nickel oxide is simply deposited on the iron oxide layer. Therefore, a successive nickel oxide growth is kinetically favourable under this condition rather than any other reaction with pre-deposited iron oxide, such as the exchange reaction between Ni^{2+} ions in solution and Fe^{2+} ions in the iron oxide lattice.

The nickel oxide deposition was carried out on pre-deposited magnetite layers directly formed with magnetite micro-particles. Fig. 4(b) shows a plot of the nickel content against the iron content in the deposits. In contrast to Fe^{2+} ions, the magnetite particles were deposited only on the boiling surface. The amount of deposited particles was much less than that formed from Fe^{2+} ions, because the concentration of magnetite particles, 0.92 μg Fe/ml, was relatively lower than that of Fe^{2+} ions, 50 μg Fe/ml, and the particulate form of iron oxide is not deposited as readily as Fe ion form is. The nickel oxide deposition increased sensitively with an increased amount of pre-deposited magnetite. These results indicate that a nickel oxide deposition could be formed inside a magnetite particle layer with a porous structure.

Based on the present experimental results, we estimated the deposition pattern of nickel oxide on pre-deposited magnetite layers. The diagram in Fig. 5(a) illustrates the nickel oxide deposition on an iron oxide layer with a dense structure, taking into account the experimental result showing that a nickel oxide deposition does not depend on the amount of pre-deposited iron oxide. Fig. 5(b) shows a possible deposition pattern to explain how a nickel oxide deposition depends on the amount of pre-deposited magnetite.

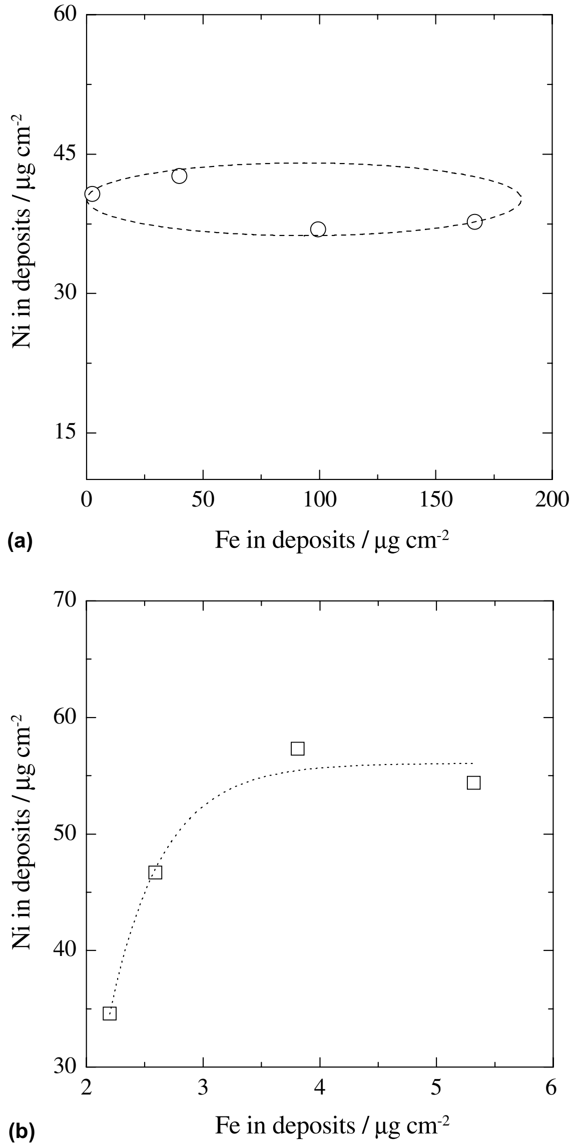

Fig. 4. (a) Effects of pre-deposited iron oxide on a nickel oxide deposition. Pre-deposited iron oxide layers were formed from Fe^{2+} ions. (b) Effect of pre-deposited iron oxide on nickel oxide deposition. Pre-deposited iron oxide layers were formed from magnetite particles.

3.4. *Effect of the Fe ion on the deposition of an iron oxide micro-particle*

In our previous work [13], iron oxide deposits were formed by the presence of Fe^{2+} ions under

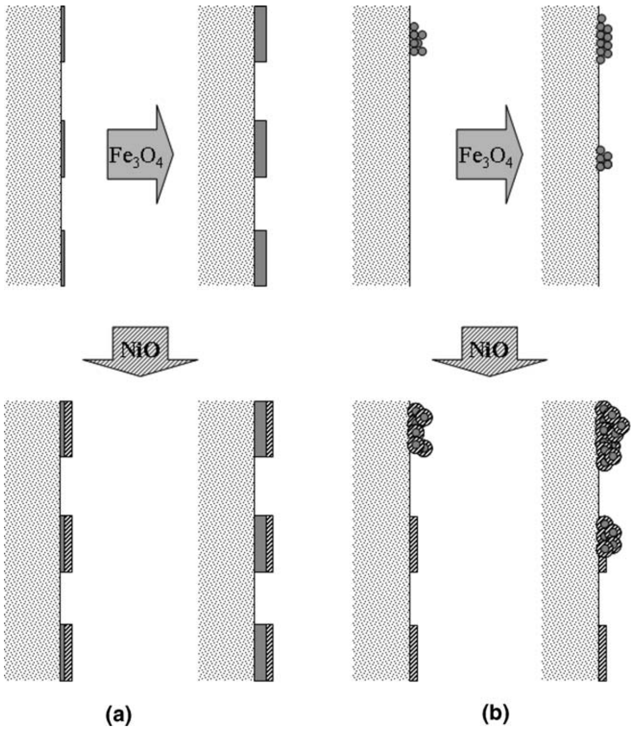

Fig. 5. Proposed schematic representation for a nickel oxide deposition on the iron oxide layers formed from (a) Fe^{2+} source and (b) magnetite particles, respectively: Dotted part, Zircaloy; Solid part, iron oxide; Hatched part, nickel oxide. The above diagrams illustrate the iron and nickel oxides deposition steps.

both non-boiling and boiling heat transfer conditions, while iron oxide micro-particles were deposited only in the boiling condition. In order to examine the effects of the Fe^{2+}ion on the deposition of iron oxide micro-particles under non-boiling conditions, we carried out iron oxide deposition tests in the following two solutions: a suspended hematite solution ([Fe] = 30 μg/ml) and a mixed solution consisting of Fe^{2+} ions ([Fe] = 50 μg/ml) and suspended hematite ([Fe] = 30 μg/ml).

Fig. 6(a) shows that no deposition layers were produced on the Zircaloy surface in the suspended hematite solution except for a ZrO_2 thin film resembling the deposits. This observation is significantly different with that under boiling heat transfer conditions. Fig. 6(b) clearly shows that the deposited layers in the mixed solution consist of a relatively distinct inner layer and a dark brown outer layer partially coated on the inner layer. The outer iron oxide layer was easily removed from the inner layer by an ultrasonic cleaning in distilled water. However, the inner layer was strongly attached to the Zircaloy surface and could only be removed by ultrasonic cleaning in 5 M HCl solution. The experimental results are summarised in Table 3.

From these results it is thought that the outer layer deposits originated from the particulate material of the suspended hematite, and the deposition of the particles was dramatically promoted by the inner oxide layer formed by Fe^{2+} ions. The particulate deposits begin to appear just after the inner layer was formed, because the characteristics of

Fig. 6. Photographs of the Zircaloy surfaces after the deposition experiments at 200 °C in (a) suspended hematite solution and (b) mixed solution consisting of Fe^{2+} ions and hematite colloidal particles.

Table 3
Effects of Fe^{2+} ions on the deposition of suspended hematite on the heat exchanging Zircaloy surface

Deposition solution (μg/ml Fe)	Amount of deposits (μg Fe/cm^2)	Layer
Suspended hematite (30)	< 0.1	–
Suspended hematite (30) + Fe^{2+} ions (50)	2.3 10.5	Outer Inner

the interaction between the suspended hematite and the Zircaloy surface becomes favourable for a deposition.

4. Conclusions

In the present work, heat treatment of Zircaloy surface with 400–500 °C steam for 4 h proved to be very effective for reducing the iron oxide deposition. It was also found that dissolved hydrogen promoted the iron oxide deposition. This was attributed to an acceleration of the water boiling and the low solubility of the iron oxide near the steam bubbles. The iron oxide layer formed from the Fe^{2+} ions did not influence a subsequent nickel oxide deposition; however, the iron oxide layer formed with magnetite particles promoted a subsequent nickel oxide deposition. It is thought that the magnetite particle layer has a porous structure, and thus a large deposition surface. The presence of Fe^{2+} ions rendered the Zircaloy surface more favourable for a deposition of the hematite colloidal particles. Our results indicate that a metal deposition on a heat transfer surface could be mitigated by the optimisation of the parameters selected in this paper.

Acknowledgement

This work was supported by the Nuclear R&D Program of the Korean Ministry of Science and Technology (MOST).

References

[1] C.J. Wood, PWR primary water chemistry guidelines: Revision 3. Electric Power Research Institute, USA, Report EPRI TR-105714, 1995.
[2] M.C. Song, K.J. Lee, Ann. Nucl. Energy 30 (2003) 1231.
[3] J. Gardner, in: Proc. Int. Conf. of Water Chem. Nuclear Reactor Systems, October 11–14, 2004, San Francisco, USA.
[4] B. Cox, J. Nucl. Mater. 336 (2005) 331.
[5] J.A. Sawicki, H.A. Allsop, J. Nucl. Mater. 240 (1996) 22.
[6] J. Blok, P. Frattini, T. Moser, in: Proc. Int. Conf. of Water Chem. Nuclear Reactor Systems, April, 22–26, 2002, Avignon, France.
[7] M.C. Song, K.J. Lee, Nucl. Eng. Des. 229 (2004) 101.
[8] M. Haginuma, S. Ono, M. Sambongi, K. Takeda, K. Tachibana, K. Ishigure, in: Proc. JAIF Int. Conf. Water Chem. Nucl. Power Plants, October, 13–16, 1998, Kashiwazaki, Japan.
[9] V.G. Kritsky, Water chemistry and corrosion of nuclear power plant structural materials, first ed., American Nuclear Society, Illinois, 1999.
[10] P.J. Millett, PWR primary water chemistry guidelines: Revision 4, Electric Power Research Institute, USA, Report EPRI TR-105714-V1R4, 1999.
[11] K.A. Burrill, in: Proc. JAIF Int. Conf. Water Chem. Nucl. Power Plants, October, 13–16, 1998, Kashiwazaki, Japan.
[12] B. Buecker, Power plant water chemistry: a practical guide, first ed., PennWell Publishing Company, Oklahoma, 1997.
[13] J. Yeon, W. Kim, Y. Park, J. Rim, Y. Jung, K. Jee, K. Choi. Research on radiochemistry and nuclear chemistry, Korea Atomic Energy Research Institute, Republic of Korea, KAERI/RR-2426/2003, 2003.